积雪草苷通过调节钙信号稳态缓解肝纤维化

王磊杰[1] 林啟浩[2] 林佳杰[2] 王佳雪[2] 庄冬瑞[2] 金园庭[1*] 闫志斌[2*]

([1]中国计量大学生命科学学院, 杭州 310018; [2]浙江理工大学生命科学与医药学院,
浙江省家蚕生物反应器和生物医药重点实验室, 杭州 310018)

摘要 肝纤维化是慢性肝病向肝硬化和肝细胞癌进展的重要过程。然而, 目前尚未有临床批准的特效药物用于治疗肝纤维化。该研究旨在探究积雪草苷的抗肝纤维化作用, 并阐明其作用机制。活化的肝星状细胞在肝纤维化的发生和发展过程中起着关键作用。在体外实验中, 积雪草苷可显著抑制人肝星状细胞系LX-2的活化、增殖和迁移; 之后对积雪草苷处理前后的肝星状细胞进行转录组测序揭示其作用机制, 结果提示积雪草苷的抗纤维化作用依赖于钙信号通路; 进一步的实验证实积雪草苷诱导胞质钙下调同时促进线粒体钙超载。此外, 积雪草苷还可促进细胞凋亡、抑制炎症和降低活性氧水平。最后, 在四氯化碳诱导的肝纤维化模型中, 积雪草苷可显著缓解肝胶原沉积和钙通路异常, 并抑制肝纤维化的发展。综上所述, 积雪草苷通过介导钙信号通路改善肝纤维化进程, 该研究为临床治疗肝纤维化疾病提供了有前景的候选化合物。

关键词 肝纤维化; 积雪草苷; 钙信号通路; 线粒体钙超载

Asiaticoside Alleviates Liver Fibrosis by Regulating Calcium Signaling Homeostasis

WANG Leijie[1], LIN Qihao[2], LIN Jiajie[2], WANG Jiaxue[2], ZHUANG Dongrui[2], JIN Yuanting[1*], YAN Zhibin[2*]

([1]*College of Life Sciences, China Jiliang University, Hangzhou 310018, China*; [2]*Zhejiang Provincial Key Laboratory of Silkworm Bioreactor and Biomedicine, College of Life Sciences and Medicine, Zhejiang Sci-Tech University, Hangzhou 310018, China*)

Abstract Liver fibrosis is a vital determinant in the development of chronic liver diseases towards liver cirrhosis and hepatocellular carcinoma. However, there are currently no approved specific agents for effectively halting liver fibrosis. Therefore, the aim of this study was to investigate the potential role of Asiaticoside in combating liver fibrosis and to elucidate the underlying mechanisms. *In vitro* experiments showed that Asiaticoside markedly inhibited the human LX-2 cells viability and migration, which are known to be participate in fibrosis development. RNA-sequencing was performed on HSCs following Asiaticoside administration, which revealed that the antifibrotic effects of Asiaticoside depend on calcium signaling pathways. Importantly, Asiaticoside induced cytosolic calcium down-regulation while mitochondrial calcium overload. In addition, Asiaticoside also promoted apoptosis, inhibited inflammation and reduced ROS (reactive oxygen species) levels. Asiaticoside significantly alleviated both hepatic collagen deposition and calcium pathways abnormalities, and inhibited the development of liver fibrosis in the CCl_4 (carbon tetrachloride)-induced mouse models. In summary, Asiaticoside ameliorated liver fibrosis by calcium signaling pathways, which provides a promising candidate for the clinical treatment of liver fibrosis.

Keywords liver fibrosis; asiaticoside; calcium signaling; mitochondrial calcium overload

收稿日期: 2024-04-22 接受日期: 2024-05-20

国家自然科学基金(批准号: 81770176、82204492)和浙江省自然科学基金(批准号: LD22H310004、LTGY24H030005)资助的课题

*通信作者。Tel: 0571-86835772, E-mail: jinyuanting@cjlu.edu.cn; Tel: 15117142783, E-mail: yanzhb15@zstu.edu.cn

Received: April 22, 2024 Accepted: May 20, 2024

This work was supported by the National Natural Science Foundation of China (Grant No.81770176, 82204492), and Zhejiang Provincial Natural Science Foundation of China (Grant No.LD22H310004, LTGY24H030005)

*Corresponding authors. Tel: +86-571-86835772, E-mail: jinyuanting@cjlu.edu.cn; Tel: +86-15117142783, E-mail: yanzhb15@zstu.edu.cn

Liver fibrosis represents an essential stage of continuous progression of liver acute or chronic liver disease, from simple injury to end-stage of liver diseases such as cirrhosis and even liver cancer, which remains a significant and global health concern due to its drastic rise incidence[1-2]. It is reported that approximately 1% to 2% of global population is affected by liver fibrosis, and no less than one million patients die worldwide every year[3]. Persistent liver fibrosis leads to excessive deposition of ECM (extracellular matrix) and replacement of liver parenchymal portions[4], breaking the normal liver physiological function. Hence, it is imperative to develop satisfactory antifibrotic drugs to slow the development of mild liver disease from progressing into a fatal condition.

As the major fibrotic effector cells, HSCs (hepatic stellate cells) play an important role in the onset and advancement of liver fibrosis. Two types of chronic liver injury, namely hepatotoxic injury and cholestatic injury, directly or indirectly activate HSC to transdifferentiate into myofibroblasts, which synthesizing a generous number of ECM and leading to escalating hepatic fibrosis[5-6]. Therefore, specific targeted intervention therapy to induce HSC inactivation will promote precision anti-fibrosis therapy.

ASIA (asiaticoside) is a natural pentacyclic triterpenoid and the main bioactive components of centella asiatica. It manifests a wide range of pharmacological properties, encompassing anti-oxidant, antidepressant, wound-healing, anti-tumor, anti-inflammatory, and anti-fibrosis[7-8]. Recent data have demonstrated that ASIA ameliorated the blood-spinal cord barrier disruption through mediating endoplasmic reticulum stress[9]. SHENG et al[10] discovered that ASIA relieved peritoneal fibrosis by inhibiting the JAK2/STAT3 signaling pathway. Studies in mammalian animal models, ASIA attenuated bleomycin-induced pulmonary fibrosis by activating cAMP and Rap1 pathways[11]. However, the mechanism of its treatment of liver fibrosis is still exist elusive.

In this research, we investigated the benefit of ASIA on LX-2 cells (a human hepatic stellate cell line) and CCl_4 induction liver fibrosis mice model, and transcriptomics was used to further detect the potential mechanisms of its therapeutic effects. Our results indicated that ASIA inhibited HSCs activation dependent on calcium signaling pathways, ultimately improved liver fibrosis.

1 Materials and methods

1.1 Cells culture

LX-2 cells, acquired from Haixing Biosciences company (TCH-C391, HyCyte™). The cells proliferate in complete medium (TCH-G391, HyCyte™). The cells were cultured in a controlled incubation environment with 5% CO_2 at a temperature of 37 °C. Upon reaching 80%-90% confluency, enzymatic hydrolysis of cells with 0.25% trypsin solution, and it is then appropriate to spread 2×10^5 cells per well in a 6-well plate subsequently. Before the experiment, the cells were subjected to a serum-free period overnight. Treated LX-2 cells with ASIA for a duration of 48 h. In the TGF-β-induced group, used a concentration of 15 ng/μL TGF-β to pretreated cells for 1 hour, At the end of pretreating, ASIA was also administered to this group for 48 h. To ensure the robustness of the data, all experiments were conducted in triplicate.

1.2 Cell viability assay

MTT assay evaluated the effect of ASIA on LX-2 cells viability and proliferation. We then plated 1×10^4 LX-2 cells per well in 96-well plates, and treated with various concentrations of ASIA treatment for a duration of 48 h. After the allotted time, we dropped 20 μL MTT solution in each well, and then incubated them at 37 ℃ for 2 h. Absorbance measured at both 490 nm and 570 nm were then recorded using a microplate reader.

1.3 Transcriptomic analysis

Cells in the exponential growth stage were evenly distributed into 9 large dishes, with a seeding density of 5×10^6 cells per dish. ASIA was added to make the final concentrations of 0, 20 and 40 μmol/L, and 3 large dishes were set for each concentration. Following 48 h of treatment, cells were digested with 0.25% trypsin for 2 min and centrifuged at 1 000 r/min for 5 min, and

1 mL of Trizol was added and placed at –80 °C. A total of three biological replicates were performed; samples were sent to Beijing Nuohe Zhiyuan Technology Co., Ltd for total RNA extraction, mRNA enrichment, and genome-wide mRNA sequencing analysis using illunima nova PE150.

1.4 Calcium flux assay

To investigate the changes in mitochondrial calcium and cytosolic calcium levels, we employed a Confocal Laser Scanning Microscope. Initially, 2×10^5 cells were inoculated in a 35 mm glass bottom cell culture dish with 1 mL fresh medium and left them in cell incubator overnight. Following this, we aspirated and discarded the medium, and washed the cells gently twice with assay buffer 1. Then added 200 μL of Fluo-4^{AM} or Rhod-2^{AM} working solution at a concentration of 4 μmol/L to the dish tank and incubated at 37 °C for 50 min. Subsequently, assay buffer 1 was carefully washed twice, and finally 1 mL assay buffer 1 was added. The corresponding Fluo-4 or Rhod-2 channels were selected according to the dye type, and 9 consecutive images were taken as the basal fluorescence of the cells at 40× objective. Following the ninth slide, the desired concentration of ASIA solution was added to the liquid level of the imaging field. The imaging process was set to capture images at a 5-second interval, resulting in a total of 300 images being acquired. This approach allowed us to monitor the dynamic changes in mitochondrial calcium and cytosolic calcium levels in response to ASIA treatment.

1.5 Mitochondrial ROS assay

Mitochondrial ROS was detected by flow cytometry CyFlow Cube 6. LX-2 cells in logarithmic phase were collected and adjust the cell density to 5×10^5 cells per well and seed in a 6-well plate (2 mL culture system). Time gradients of 0, 1, 3, and 6 h were established, during which 40 μmol/L ASIA was added to each well, and then the plate was placed in the incubator at 37 ℃. After culturing to the specified time, collect the cells in a centrifuge tube and centrifuged at 1 000 r/min for 5 min, 0.5 mL culture medium was reserved to resuspend the cell pellet, and 0.5 mL MitoSOX dye was added to each tube to fully mix; placed in the incubator and inverted every 3-5 min to mix well. After washing the cells with PBS, 1 mL PBS was used to resuspend and prepare for detection; FL2 channel was utilized by flow cytometry.

1.6 Cytosolic ROS assay

Fluorescence inverted microscopy was employed to detect cytosolic ROS. Collected LX-2 cells in the logarithmic growth phase and then inoculated into 6-well cell culture plates, with a density of 5×10^5 cells per well in 2 mL of fresh medium. ASIA treatment was administered at a concentration of 20 μmol/L, with four different points in time: 0, 1, 3, and 6 h. To measure the cytosolic ROS, DCFH-DA was diluted 1:1 000 with serum-free culture medium to achieve 10 μmol/L. The cell culture medium was discarded, and added 1 mL of the diluted DCFH-DA solution in a dark environment. Following a 20-minute incubation at 37 °C, cells were washed three times with serum-free medium to ensure removal of DCFH-DA that without entering cells. Excitation wavelength of 488 nm and an emission wavelength of 525 nm were used, the fluorescence intensity was measured before and after stimulation at each time point.

1.7 Western blot

Cells or tissues were collected at the specified time points, then lysed with radio-immunoprecipitation assay buffer (RIPA; Servicebio, Wuhan, China) supplemented with phenyl-methylsulfonyl fluoride (PMSF; Servicebio, Wuhan, China) at a ratio of 100:1 to ensure protein stability. Determined the protein concentration by a bicinchoninic acid (BCA; Solarbio, Beijing, China) protein assay kit, and the required protein samples were prepared accordingly. Follow by the protein samples electrophoresis experiments were performed in sodium dodecyl sulfate-polyacrylamide gels (SDS-PAGE) at appropriate concentrations. Subsequently, transferred the proteins onto polyvinylidene difluoride membranes (PVDF; Millipore, Germany). Using 5% (*w*/*v*) skimmed milk to block the membranes for 2 h at room temperature, and then the primary antibodies was incubated overnight at 4 °C. Horseradish peroxidase-conjugated (HRP) secondary antibodies (Bioworld, BS13278, 1:10 000) were used for incubation under

room temperature for 2 h. The protein bands were detected using an electrochemilum- minescence (ECL; ChampChemi 910 Plus, Sagecreation) detection system. Utilizing Image J software (Bio-Rad, USA) to measure the optical density of the bands and to normalize to GAPDH (Bioworld, AP0066, 1:10 000) or β-actin (Bioworld, AP0060, 1:10 000). The primary antibodies that used in this research including: α-smooth muscle actin (α-SMA, HUABIO, 1:1 000), collagen type I alpha 1 (Col1a1, HUABIO, ET1609-68, 1:1 000), PDGF (HUABIO, ET1605-20, 1:1 000), IL-1β (ABclonal, P01584, 1:1 000), IL-6 (Bioworld, BS6419, 1:1 000), actived-caspase-3 (Bioworld, BS7004, 1:1 000), caspase-3 (Bioworld, BS1518, 1:1 000) and Anti-Calmodulin (Calm; HUABIO, ET1606-46, 1:1 000).

1.8 RT-qPCR

Using TransZol Up reagent (Transgen, Beijing, China) to extract tissues and cells, and then the RNA content was quantified by a Nanophotometer P330 Spectrophotometer (Implen, US). Subsequently, 1 μg of total RNA was utilized for cDNA synthesis, performed using a reverse transcription kit (Monad, Suzhou, China). The resulting cDNA was amplified by the SYBR Green qPCR Mix kit (Monad, Suzhou, China). Using the $2^{-\Delta\Delta Ct}$ method to determine the target genes relative expression levels, with normalization to the expression level of *GAPDH*. For reference, the primer sequences used are provided in Table 1.

1.9 Animals and experimental protocols

Purchasing male C57BL/6 mice (6-week-old) from Charles River (Hangzhou, China) and acclimated to laboratory conditions for 1 week prior to the experiment. The mice were placed in a SPF (specific pathogen free) animal facility for a 12-hour light/dark cycle and maintained at appropriate temperature and humidity levels [(25±1) °C, (55±5)%, respectively]. Bedding was regularly changed, and the mice had free access to food and water during the entire process of the experiment, all animal experiments were approved by the Experimental Animal Ethics Committee of Zhejiang Sci-Tech University (Ethics review approval number: 202303001).

In order to establish liver fibrosis model, the mice were intraperitoneally injected with 20% CCl_4 (*v*/*v*) dissolved in corn oil at a dose of 5 mL/kg twice a week, on fixed days (Monday and Thursday), The mouse liver fibrosis model constructing add up to 6 weeks. Under the same volume and frequency, control mice were injected with corn oil alone. At the third week, arbitrarily divided the mice into three groups (n=6 per group) using the fol-

表1 RT-qPCR引物序列

Table 1 Primers for RT-qPCR

基因名称 Gene	引物序列(5′→3′) Primer sequence (5′→3′)
ADRA1D-F	TTA TGG CCG TGG CAG GTA AC
ADRA1D-R	GCC AGG TTC ACG ATG AAA TAG TT
EGF-F	TCC TCA CCC GAT AAT GGT GGA
EGF-R	CCA GGA AAG CAA TCA CAT TCC C
FGF1-F	GCC CTG ACCGAGAAGTTTAATC
FGF1-R	CCC CGT TGC TAC AGT AGA GG
GRIN2A-F	TCA TGC AGG ATT ATG ACT GGC A
GRIN2A-R	TGT GGT CTT GAC GAA GCT GAT
NTRK3-F	ACG AGA GGG TGA CAA TGC TG
NTRK3-R	CCA GTG ACT ATC CAG TCC ACA
OXTR-F	CTG CTA CGG CCT TAT CAG CTT
OXTR-R	CGC TCC ACA TCT GCA CGA A
GAPDH-F	AAC TTT GGC ATT GTG GAA GG
GAPDH-R	CAT CGA AGG TGG AAG AGT GG

lowing methods: (a) Control group was intraperitoneally injected with corn oil, (b) 20% CCl_4-treated group, (c) ASIA-treated (20 mg/kg) group. The above three groups were also given the same amount of corn oil, 20% CCl_4 or ASIA solution intraperitoneally injection daily. Six weeks later, all mice were sacrificed, followed by rapid collection of blood samples and liver tissues, supernatant serum was taken after blood centrifugation, and liver tissues were washed with PBS and photographed. All tissues placed at –80 °C for preservation.

1.10 Biochemical analyses

Liver function markers, including AST (aspartate aminotransferase) and ALT (alanine aminotransferase), were assessed using assay kits obtained from Nanjing Jiancheng Bioengineering Institute (Nanjing, China).

1.11 Histological analysis

The liver tissue was fixed with 4% neutral paraformaldehyde solution and cut into 4-μm slices after paraffin embedding. Then the slices were dewaxed in graded xylene and rehydrated in graded alcohol. Subsequently, the liver tissues were stained with H&E (hematoxylin-eosin), as well as Sirius red and Masson staining solution. Microscope was used to observe histological changes in a randomly selected field of view.

1.12 IHC (immunohistochemistry)

Liver tissue samples, fixed with 4% neutral paraformaldehyde solution and cut into 4-μm slices after paraffin embedding. The following procedures were performed: (a) The tissue samples were baked, deparaffinized in xylene, and hydrated in ethanol. (b) Endogenous peroxidase was blocked in a dark room at room temperature for 10 min using citrate buffer containing 3% hydrogen peroxide. (c) The sections were removed from the beaker, and added 1% BSA (bovine serum albumin) solution dropwise to completely cover the tissue. And then the sections were incubated under 37 °C for 1 h. (d) Antibodies were diluted in 1% BSA (1:200, *v*/*v*) and incubated with the sections overnight under 4 °C. (e) Next day, the sections were allowed to reach room temperature and incubated with the secondary antibody (1:200, *v*/*v*) under room temperature for 2 h. (f) Detected protein expression using DBA (3,3-diaminobenzidine) staining, and the nuclei were observed using hematoxylin staining. (g) Finally, the sections were photographed using a microscope.

1.13 Statistical analyses

Each set of experiments was repeated independently more than three times, All data were expressed as $\bar{x}\pm s$, *t* test and ANOVA were used for significance statistics, and differences in means of the two samples could be compared using T test when the sample size was small and conformed to a normal distribution. One-Way analysis of variance (ANOVA) is a statistical test that can be employed when there are multiple groups of samples that obey a normal distribution and have equal variances. It allows for the assessment of significant differences in the means among these groups. Samples may be analyzed using a Mann-Whitney test when they fail to meet the normal distribution or homogeneity of variance conditions. Significant differences $^{*}P<0.05$, $^{**}P<0.01$, $^{***}P<0.001$, $^{\#\#}P<0.01$, $^{\#\#\#}P<0.001$ indicate significant data, ns: no significant. Prism Graph software was used for drawing.

2 Results

2.1 ASIA inhibits the activation of LX-2 cells

The excessive proliferation of activated hepatic stellate cells is a crucial factor for promoting liver fibrosis. In this study, we studied the impact of ASIA on cell proliferation, and fibrotic key markers in LX-2 cells. In order to assess the impact of ASIA on cell proliferation, LX-2 cells were managed by ASIA that dissolve into various concentrations for 48 h. The relative living rate of the cells was measured using the MTT assay. As shown in Fig.1A, the viability of LX-2 cells decreased in a concentration-dependent manner in the ASIA concentration range of 0-50 μmol/L. Furthermore, we examined the expression of fibrotic key markers, including α-SMA, Col1a1, and PDGF using Western blot assays. As shown in Fig.1B, treatment with ASIA notably reduced α-SMA, Col1a1, and PDGF proteins expression level in LX-2 cells compared to the control group. We also conducted the cell scratch assay to investigate the impact of ASIA on LX-2 cells migra-

tion. As illustrated in Fig.1C and Fig.1D, cells treated with ASIA exhibited a significant decrease in migration over time, with a more pronounced effect observed at higher drug concentrations. It indicated that the migration ability of LX-2 cells was significantly inhibited by ASIA. Our results suggest that ASIA inhibits LX-2 cells activation and attenuates liver fibrosis progression.

2.2 Transcriptomic analysis of the mechanism of ASIA inhibited LX-2 cells activation

To explore the specific mechanism by which ASIA inhibited LX-2 cells proliferation, we performed transcriptome sequencing of LX-2 cells after ASIA treatment. KEGG pathway analysis of the down-regulated differentially expressed genes showed that these genes were significantly enriched in calcium signaling pathway (Fig.2A). Genes enriched in calcium signaling pathways were selected for heat map presentation (Fig.2B), including *ADRA1D*, *EGF*, *FGF1*, *GRIN2A*, *NTRK3*, *OXTR*. This result was subsequently verified by RT-qPCR (Fig.2C). These data suggest that ASIA inhibited LX-2 cells activation closely related to cal-

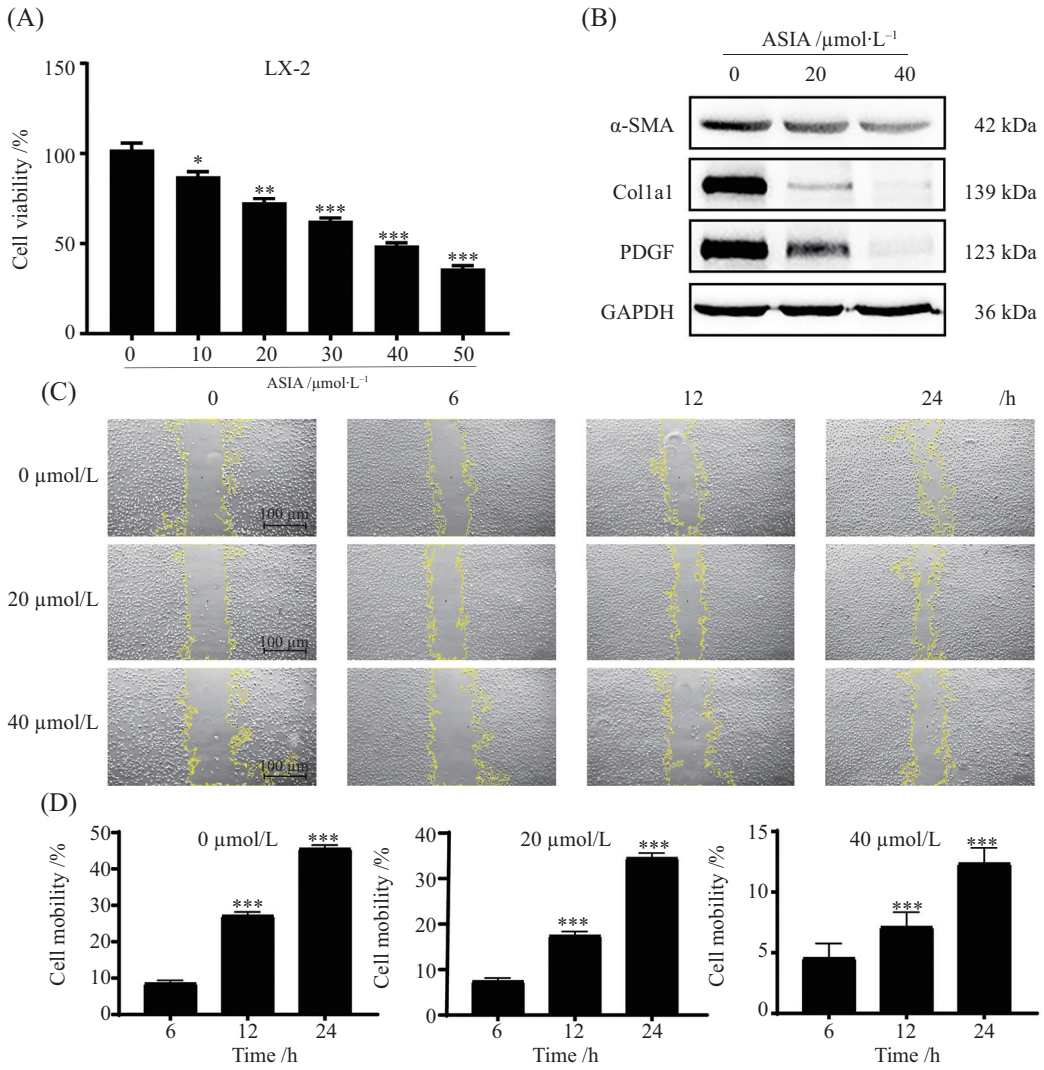

A: MTT实验检测LX-2细胞经积雪草苷(0~50 μmol/L)处理后的细胞活力; B: Western blot实验检测LX-2细胞经积雪草苷处理后纤维化相关蛋白表达变化; C、D: 划痕实验检测LX-2细胞经积雪草苷处理后迁移能力; *P<0.05, **P<0.01, ***P<0.001, ASIA组与Control组比较。

A: cell viability in LX-2 cells post-ASIA exposure (0-50 μmol/L) was assessed via MTT assay; B: post-treatment of LX-2 cells with ASIA, fibrosis-associated proteins were tested via Western blot and subjected to statistical analysis; C,D: the migration capability of LX-2 cells with ASIA treatment was evaluated using a scratch assay, followed by statistical analysis; *P<0.05, **P<0.01, ***P<0.001, ASIA group compared with Control group.

图1 积雪草苷抑制LX-2细胞活化

Fig.1 ASIA suppresses LX-2 cells activation

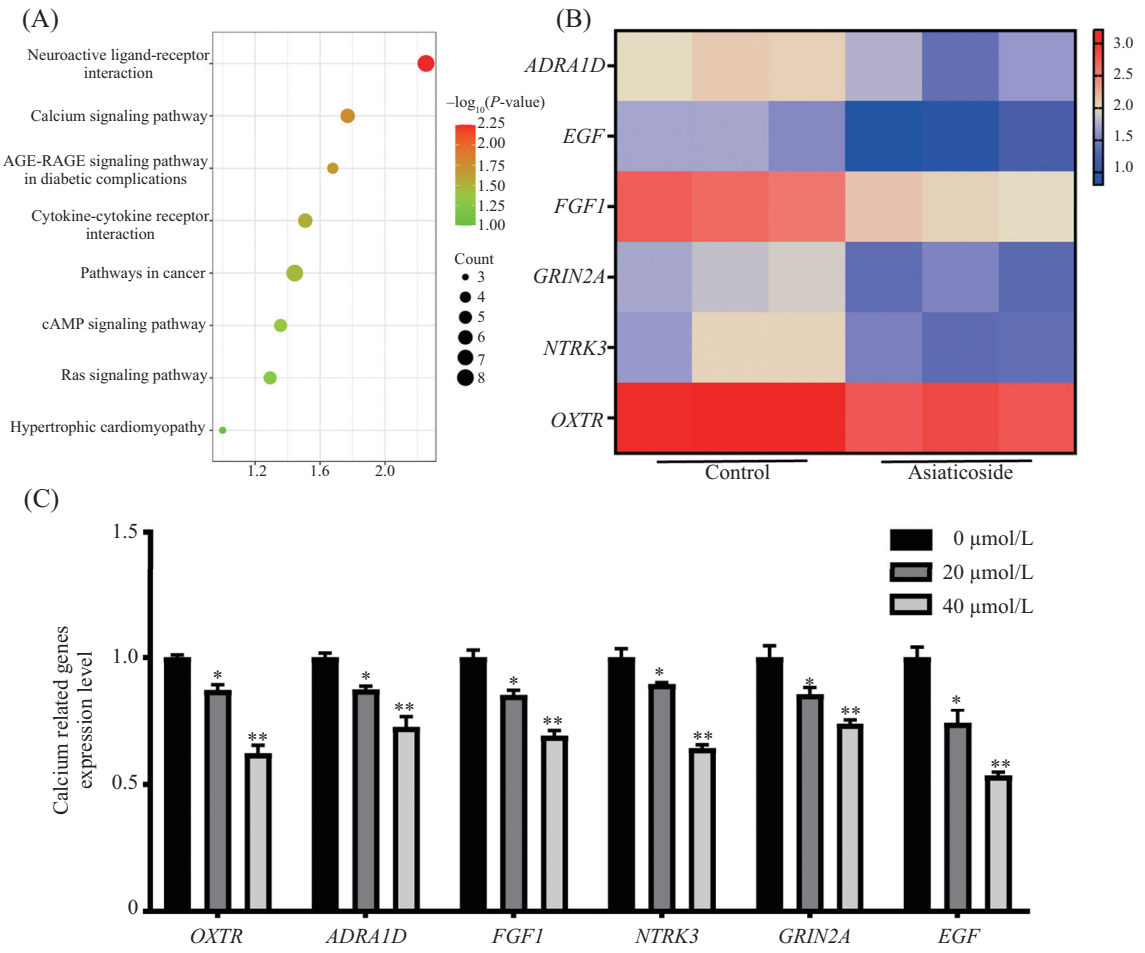

A: LX-2细胞经0和40 μmol/L积雪草苷处理48 h后转录组测序, 随后进行KEGG通路富集分析; B: 钙流相关基因热图; C: RT-qPCR验证钙信号通路相关基因; *P<0.05, **P<0.01, ASIA组与Control组比较。

A: LX-2 cells, post 48 h treatment with 0 and 40 μmol/L ASIA and subsequent transcriptome sequencing, underwent KEGG pathway enrichment analysis; B: the heat map displays genes associated with the calcium signaling pathway; C: RT-qPCR validated genes involved in calcium signaling pathway; *P<0.05, **P<0.01, ASIA group compared with Control group.

图2 积雪草苷抑制LX-2细胞活化的转录组学分析

Fig.2 Transcriptome mechanism study in ASIA-inhibited LX-2 cells activation

cium signaling pathway.

2.3 ASIA inhibits the activation of HSC cells dependent on calcium signaling pathways

Maintaining cellular homeostasis relies on the regulation of Ca^{2+} flux, which is closely related to the HSC cells activation. Based on this, we first investigated the expression changes of Calm, a calcium-associated proteins, in LX-2 cells after ASIA treatment using Western blot assay. As depicted in the Fig.3A, the expression of Calm was significantly decreased in the treatment group compared with the control group. Subsequently, we utilized cytosolic and mitochondrial calcium fluorescent probes to detect changes in intracellular calcium content after treatment with ASIA for different time periods by laser scanning confocal microscopy. The results of cytosolic calcium content change are presented in the Fig.3B and Fig.3D. Addition of ASIA at a concentration of 40 μmol/L to LX-2 cells displayed a rapid and notable decrease in cytosolic calcium content over a short period of time, which showed a slow decreasing trend after 1 000 s. Mitochondrial calcium content change results are shown in the Fig.3C and Fig.3E, where treatment with 40 μmol/L ASIA induced a substantial increase in mitochondrial calcium content, peaking at 1 000 seconds and gradually decreasing thereafter. These findings imply that ASIA causes Ca^{2+} to flow from the cytosol into mitochondria. To further clarify the effect of Ca^{2+} in HSC cells activation, we

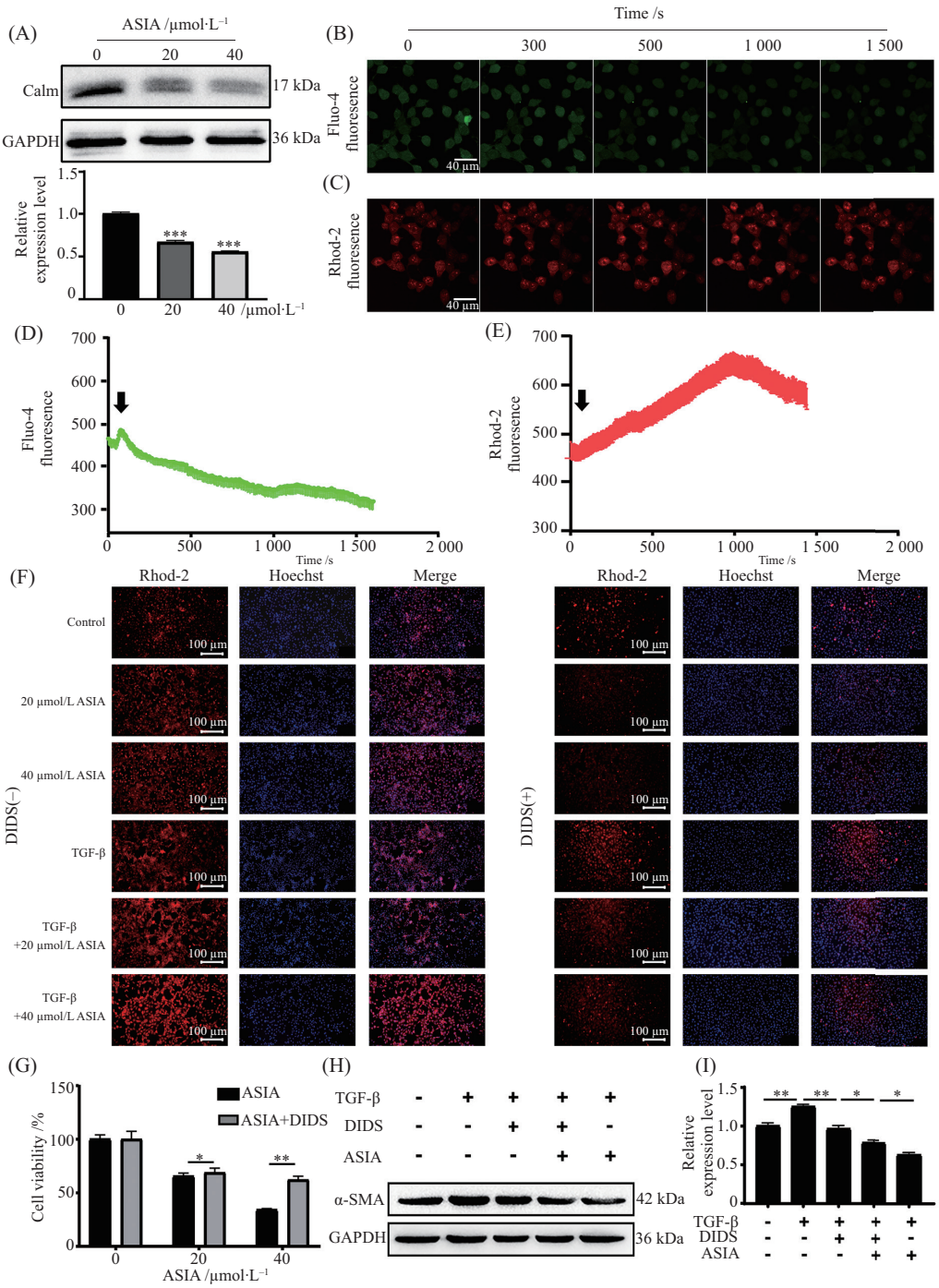

A: Western blot检测经积雪草苷处理后LX-2细胞中Calm蛋白表达变化, 并进行统计分析; B、D: LX-2细胞经40 μmol/L积雪草苷处理后, 激光共聚焦检测胞质钙变化, 并进行统计学分析(黑色箭头表示给药时间); C、E: LX-2细胞经40 μmol/L积雪草苷处理后, 用激光共聚焦显微镜检测线粒体钙变化, 并进行统计学分析(黑色箭头表示给药时间); F: 荧光倒置显微镜观察各组线粒体钙的变化; G: MTT检测DIDS(线粒体钙通道阻滞剂)对积雪草苷处理后的LX-2细胞活力的影响; H、I: Western blot检测各组α-SMA蛋白表达情况, 并进行统计学分析; *P<0.05, **P<0.01, ***P<0.001, ASIA组与Control组比较。

A: the expression of Calm protein in LX-2 cells treated with ASIA was investigated by Western blot and statistically analyzed; B,D: LX-2 cells, treated with 40 μmol/L ASIA, were imaged for cytoplasmic calcium variations using confocal microscopy, followed by statistical analysis (Black arrow indicates drug administration time); C,E: LX-2 cells, treated with 40 μmol/L ASIA, were imaged for mitochondrial calcium variations using confocal microscopy, followed by statistical analysis (Black arrow indicates drug administration time); F: fluorescence inverted microscopy captured mitochondrial calcium variations post-treatment with 20 μmol/L, 40 μmol/L ASIA, TGF-β, TGF-β+20 μmol/L ASIA, and TGF-β+40 μmol/L ASIA, with and without DIDS conditions; G: MTT assay for assessing the effect of DIDS (mitochondrial calcium channel blocker) on the viability of LX-2 cells post-ASIA treatment; H,I: Western blot analysis was conducted to assess α-SMA protein expression following treatment with TGF-β, TGF-β+DIDS, TGF-β+DIDS+ASIA, and TGF-β+ASIA, with subsequent statistical analysis; *P<0.05, **P<0.01, ***P<0.001, ASIA group compared with Control group.

图3 积雪草苷通过钙信号通路抑制HSC活化

Fig.3 ASIA suppresses HSC activation via calcium signaling pathway

used DIDS (mitochondrial calcium channel blocker) to pretreat LX-2 cells followed by ASIA, the results of fluorescence inverted microscopy showed that red fluorescence increased prominently after TGF-β induction, and increased further after ASIA treatment in a concentration-dependent manner. Compared with TGF-β induction, red fluorescence was noticeably weaker in the group without TGF-β induction, and also increased in a concentration-dependent manner after ASIA treatment (Fig.3F). Then we investigated whether ASIA induced cells death by increasing of calcium concentration in mitochondria. MTT assay shown that DIDS pretreatment significantly reversed ASIA-induced cells death (Fig.3G). Western blot showed that TGF-β-induced promotes α-SMA expression level, which was prominently inhibited by ASIA treatment, after combination with DIDS, α-SMA expression increased (Fig.3H and Fig.3I). The above results indicate that ASIA inhibits the activation of HSC cells through mitochondrial calcium overload.

2.4 ASIA induces mitochondrial oxidative stress and promotes apoptosis of LX-2 cells

Previously we showed an apparent decrease in cytosolic calcium content in LX-2 cells after addition of ASIA by confocal laser scanning microscopy. It is well-known that Ca^{2+} and ROS are multifunctional signaling molecules that coordinate pathophysiological processes, and they interact with each other[12]. To explore the impact of ASIA on intracellular ROS levels, we utilized loaded DCFH-DA probes to detect intracellular ROS levels. Results are depicted in Fig.4A. Intracellular ROS levels were clearly lower in LX-2 cells treated with ASIA compared to controls. It is well-established that alterations in ROS level plays an important role in the development of inflammatory responses[13]. To explore the potential against inflammatory activity of ASIA *in vitro*, we assessed the expression of IL-1β and IL-6. Remarkably, comparing to the control group the expression of IL-1β and IL-6 in ASIA-treated cells was suppressed (Fig.4B and Fig.4C). These results reveal that ASIA exerts its anti-inflammatory effects, thereby potentially preventing the progression of liver fibrosis.

Mitochondrial calcium overload causes abnormal fluctuations of mitochondrial ROS, and we detected the changes of mitochondrial ROS after ASIA treatment by flow cytometry. Mitochondrial ROS levels rose sharply within 1 h of ASIA treatment (Fig.4D and Fig.4E). Given the crucial role of increased mitochondrial ROS in promoting apoptosis, we further investigated the apoptotic effects of ASIA treatment on LX-2 cells. Western blot analysis was employed to assess apoptotic marker proteins expression level changes, specifically caspase3, actived-caspase3. Notably, the expression of actived-caspase3 was significantly enhanced, while caspase3 expression showed a slight decrease (Fig.4F and Fig.4G). To explore whether ASIA inhibited HSC cells activation by promoting apoptosis, we conducted MTT assays to evaluate LX-2 cells proliferation after treatment with the apoptosis inhibitor Z-VAD-FMK. As depicted in Fig.4H, the proliferation activity of cells pretreated with Z-VAD-FMK was visibly enhanced which compared to the control group. These results suggest that apoptosis inhibitor Z-VAD-FMK can reverse death caused by ASIA treatment of LX-2 cells, further certified ASIA induced apoptosis in LX-2 cells. These data demonstrate that ASIA treatment triggered mitochondria-mediated apoptosis in LX-2 cells.

2.5 ASIA has hepatoprotective effects

We investigated the hepatoprotective effects of ASIA in mice model of CCl_4-induced liver fibrosis (Fig.5A). Anatomical examination of the livers revealed that CCl_4-induced mice exhibited a lighter color and a fat layer on the surface compared to the Oil group. However, these pathological changes were reversed following ASIA treatment. Histological analysis of the mouse liver tissue using HE staining showed that the Oil-treated control group exhibited intact liver tissue structure with radial arrangement of hepatic cords, no fibrous hyperplasia, or inflammatory cell infiltration. In contrast, the CCl_4-treated group showed extensive eosinophilic degeneration, and marked lymphocytic infiltration. Notably, ASIA treatment alleviated mitigated inflammatory cell infiltration (Fig.5B). Monitor-

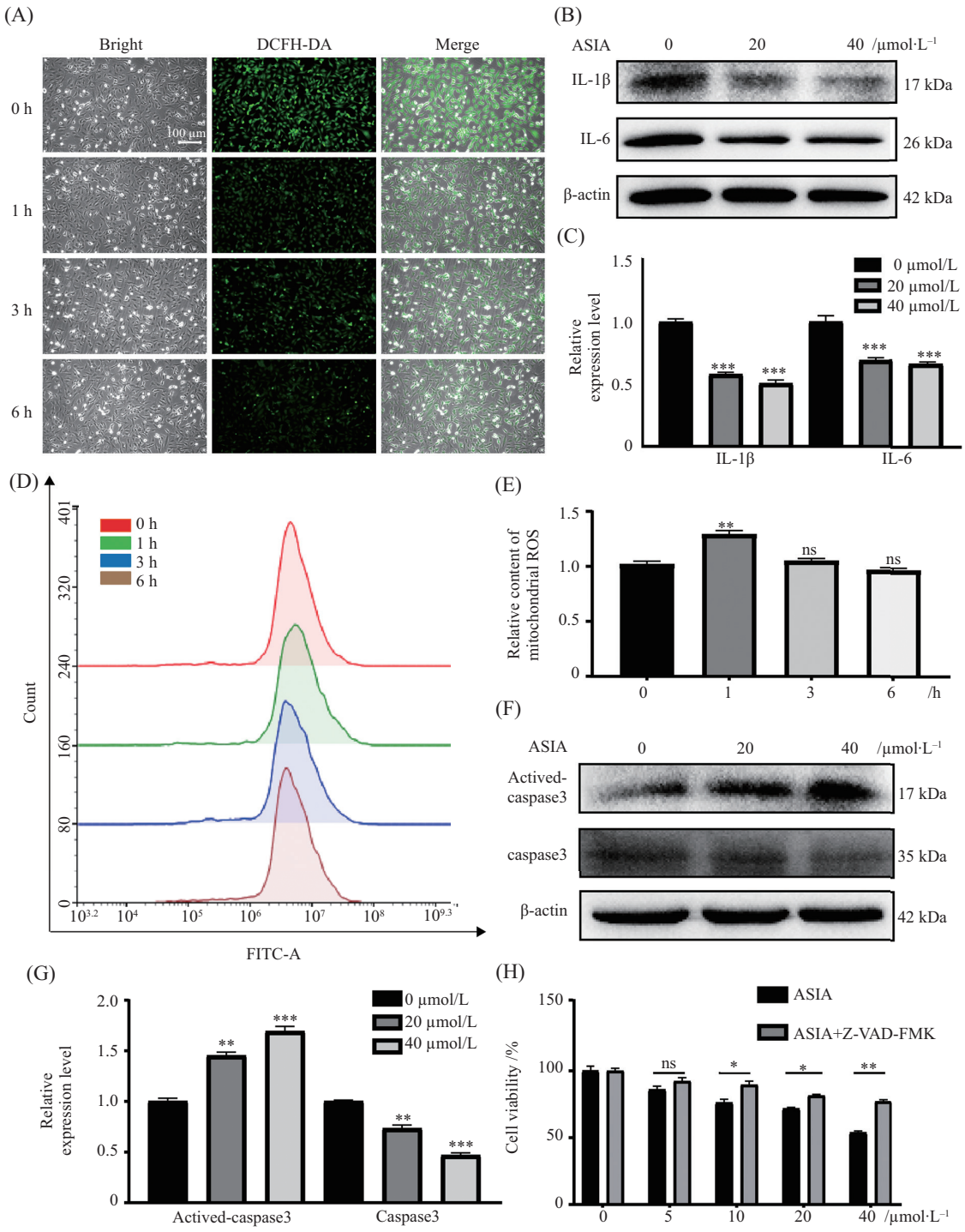

A: 荧光倒置显微镜观察不同时间点的胞质活性氧变化; B、C: Western blot检测经积雪草苷处理后IL-1β和 IL-6蛋白表达情况, 并进行统计学分析; D、E: 流式细胞术检测经40 μmol/L积雪草苷处理不同时间点线粒体ROS的变化, 并进行统计学分析; F、G: Western blot检测经积雪草苷处理后凋亡蛋白active-caspase3和caspase3蛋白表达的变化, 并进行统计分析; H: MTT检测凋亡抑制剂Z-VAD-FMK逆转积雪草苷对LX-2的增殖抑制作用; *P<0.05, **P<0.01, ***P<0.001, ns: 没有显著性, ASIA组与Control组比较。

A: detection of ROS variations at different time points using DCFH-DA probe loading, Captured by an inverted fluorescence microscope; B,C: Western blot detected IL-1β and IL-6 protein expression changes after treatment with ASIA, and statistical analysis was performed; D,E: flow cytometry detected the changes of mitochondrial ROS after treatment with 40 μmol/L ASIA at different time points, and statistical analysis was performed; F,G: Western blot detected changes in apoptotic protein actived-caspase3 and caspase3 protein expression after treatment with ASIA, and statistical analysis was performed; H: MTT assay detected apoptosis inhibitor Z-VAD-FMK reverse the effect of ASIA on LX-2 inhibition of proliferation; *P<0.05, **P<0.01, ***P<0.001, ns: no significant, ASIA group compared with Control group.

图4 积雪草苷诱导线粒体氧化应激, 促进LX-2细胞凋亡

Fig.4 ASIA induces mitochondrial oxidative stress and promoted apoptosis in LX-2 cells

ing of mice body weights revealed no remarkable differences within liver-to-body weight ratios among the three groups (Fig.5C). To further understand the effect of ASIA on liver function, we measured the enzyme activities of ALT and AST in mice serum. The results said CCl_4-induced led to a significant increase in ALT and AST levels compared to the Oil group. However, treatment with ASIA brought about a notable improvement in ALT and AST levels. These findings demonstrated that in mice with CCl_4-induced liver fibrosis, ASIA improves liver function (Fig.5D and Fig.5E). These data demonstrated that ASIA has hepatoprotective properties in mice model of liver fibrosis induced by CCl_4.

2.6 ASIA alleviates CCl_4-induced liver fibrosis in mice

In order to evaluate the impact of ASIA on intra-

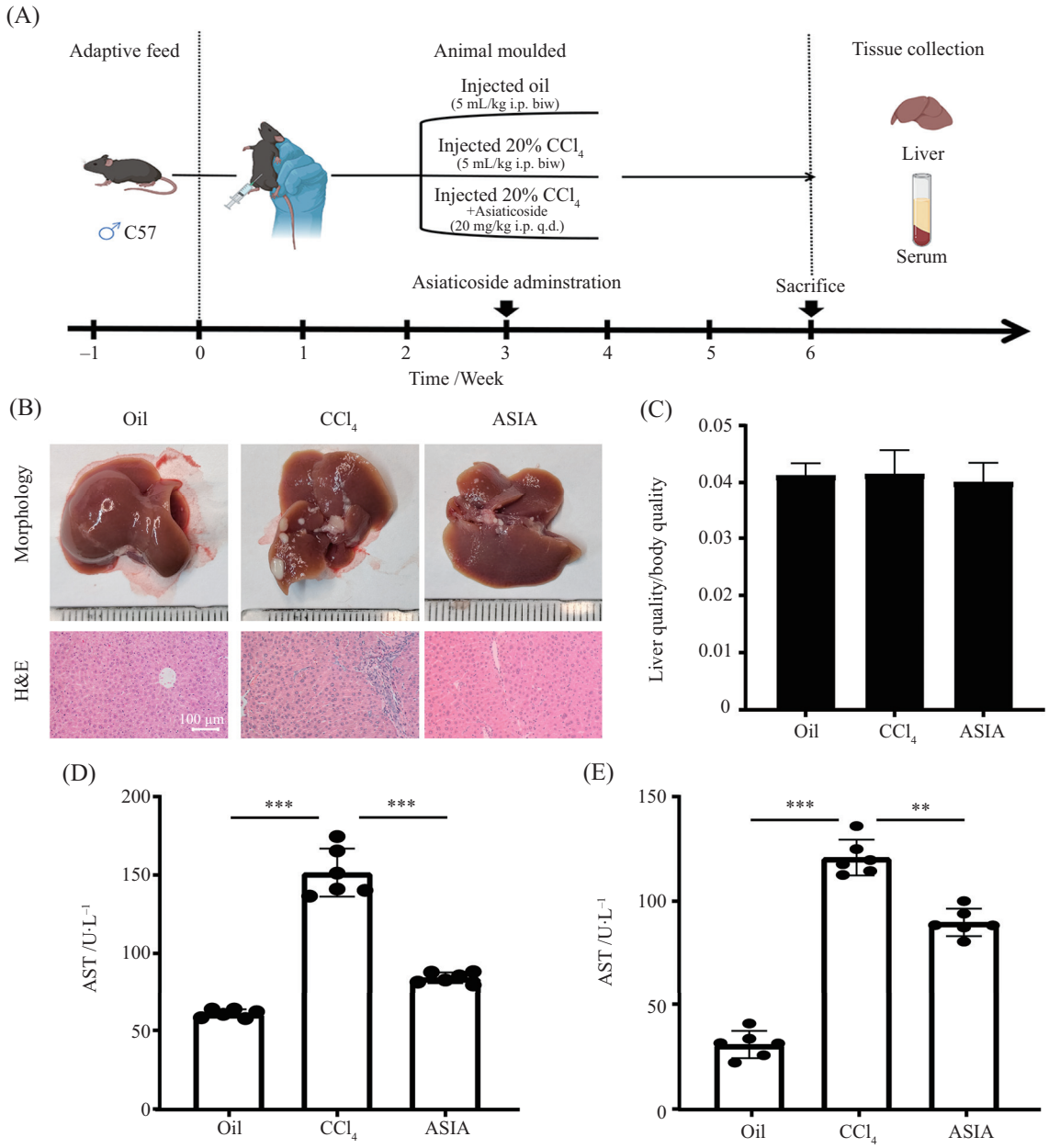

A: 动物实验流程图; B: 肝脏大体形态及HE染色; C: 小鼠肝脏体质量比; D: 血清谷丙转氨酶水平(n=6); E: 血清谷草转氨酶水平(n=6); $^{**}P$<0.01, $^{***}P$<0.001。

A: flow chart of animal experiment; B: liver gross morphology and HE staining images; C: the liver-to-body weight ratio in mice; D: serum ALT levels (n=6); E: serum AST levels (n=6); $^{**}P$<0.01, $^{***}P$<0.001.

图5 积雪草苷具有肝保护作用

Fig.5 ASIA exhibit liver-protective properties

hepatic collagen deposition, we performed Sirius red staining and Masson staining. The Sirius red staining shown in Fig.6A demonstrated that the liver tissue from the Oil group showed no significant collagen deposition. However, after CCl_4 induction, a substantial amount of collagen fibers was deposited in the portal areas and interlobular septa of liver tissues in the CCl_4-induced group. Remarkably, in the ASIA group, there was a notable reduction in collagen fiber deposition when compared with the model group. Similarly, the Masson staining results also showed that ASIA can improve liver fibrosis significantly (Fig.6A). Furthermore, we assessed the expression of liver fibrosis markers through IHC and Western blot. The IHC staining results demonstrated low positive expression levels of α-SMA and Col1a1 proteins in the liver tissue of the Oil group. In contrast, the CCl_4 group exhibited increased expression levels of α-SMA and Col1a1 in the cytoplasmic regions of fibrous septa in the portal area and sinusoidal fibroblasts near the fibrous septa. However, after ASIA treatment, the positive expression levels of α-SMA and Col1a1 in the liver tissue were significantly alleviated (Fig.6C and Fig.6D). Additionally, Western blot detects the expression changes of α-SMA, IL-1β, IL-6 and Calm at the animal level. The results showed that the expression of α-SMA, IL-1β, IL-6 and Calm increased significantly after induction with CCl_4, and treatment with ASIA decreased their expression (Fig.6E-Fig.6J). These findings suggest that ASIA alleviate intrahepatic collagen deposition in mice with liver fibrosis.

3 Discussion

Natural products derived from traditional Chinese medicine have been an important source of new drug development. In the current study, we found that ASIA, a triterpenoid extracted from centella asiatica, induced mitochondrial oxidative stress and apoptosis of LX-2 cells, and exhibited anti-inflammatory activity, as well as the down-regulated expression of intracellular inflammatory cytokines, thereby inhibiting HSC activation. Further mechanistic studies have highlighted the role of the calcium signaling pathway in the inactivation of HSC induced by ASIA (Fig.7). Moreover, ASIA treatment eased the liver fibrosis mice's symptoms which induced by CCl_4. Our work suggest ASIA has tremendous potential as a drug candidate in the fight against liver fibrosis becomes increasingly evident.

Centella asiatica, a common herb in southern China, South Asia and Southeast Asia. it has been used for centuries to treat a series of complains, including skin disorders, wound healing, chronic venous insufficiency[14]. With the development of medicinal chemistry, a variety of active components of Centella asiatica have been isolated and extracted. As the main active ingredient, ASIA possess anti-inflammatory, anti-microbiological, anti-oxidant and wound healing properties[15]. A recent study reported that ASIA showed cardioprotection against diabetic cardiomyopathy by activating AMPK/Nrf2 pathway[16]. XIA et al[17] analyzed the anti-triple-negative breast cancer effect of ASIA and found that it blocked P2RX7-mediated TGF-β/SMAD signaling pathway to inhibit epithelial-mesenchymal transition via motivating PPARG expression. Emerging research have suggested that the potential role of ASIA in liver disease. An early study from Wan's group demonstrated that ASIA has obviously hepatoprotective effects on liver injury mice model which induced by lipopolysaccharide/D-galactosamine[18]. In subsequent research, the same group found that it exerted antipyretic and anti-inflammatory effects by up-regulating the expression of heme oxygenase-1 protein in rat treated by LPS[19]. Another study revealed that ASIA inhibited the hepatitis B virus replication both *in vivo* and *in vitro*[20]. Several investigations have provided strong evidence that ASIA played an anti-fibrosis role on multiple organs, such as peritoneal fibrosis[10], kidney fibrosis[21], and pulmonary fibrosis[11]. Here, our data showed that ASIA prevented hepatic stellate cells activation and alleviated CCl_4-induced liver fibrosis. We provide promising compounds for the treatment of liver fibrosis. Since there are many kinds of cells in the liver, metal

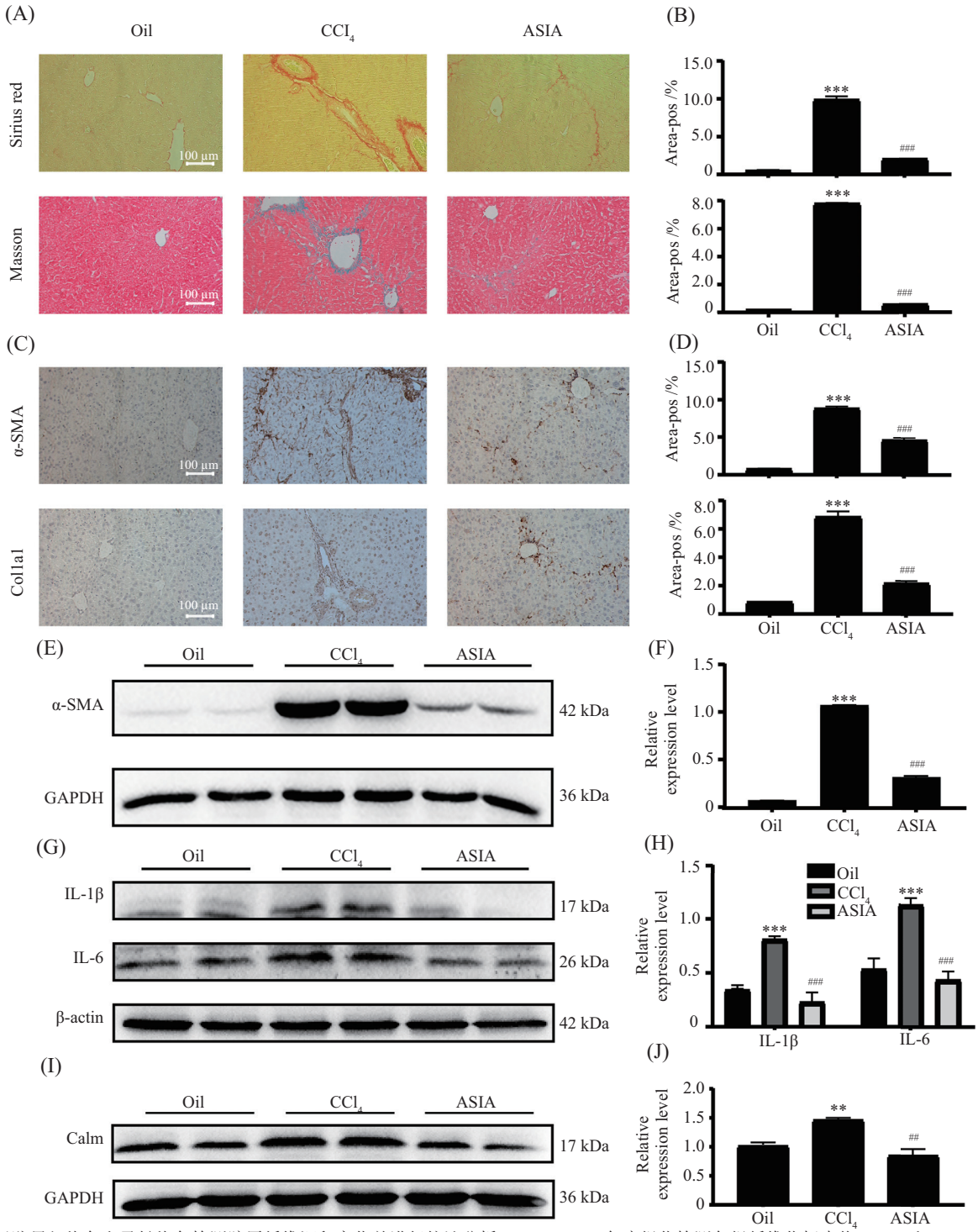

A、B: 天狼星红染色和马松染色检测胶原纤维沉积变化并进行统计分析(n=6); C、D: 免疫组化检测各组纤维化标志物α-SMA和Col1a1的表达变化并进行统计分析(n=6); E、F: Western blot实验检测纤维化标志蛋白α-SMA和Col1a1表达变化并进行统计分析(n=3); G、H: Western blot实验检测IL-1β和IL-6表达变化并进行统计分析(n=3); I、J: Western blot实验检测Calm蛋白表达变化并进行统计分析(n=3); *P<0.05, ***P<0.001, CCl4组与Oil组比较; $^{\#\#}P$<0.05, $^{\#\#\#}P$<0.001, ASIA组与Oil组比较。

A,B: the collagen fiber deposition change was detected by Sirius red staining and Masson staining and conducted statistical analysis (n=6); C,D: the expression of fibrosis marker proteins α-SMA and Col1a1 changes was detected by IHC and conducted statistical analysis (n=6); E,F: the expression of fibrosis marker proteins α-SMA and Col1a1 changes were detected by Western blot and conducted statistical analysis (n=3); G,H: the expression of IL-1β and IL-6 changes were detected by Western blot and conducted statistical analysis (n=3); I,J: the expression of Calm change was detected by Western blot and conducted statistical analysis (n=3); *P<0.05, ***P<0.001, CCl4 group compared with Oil group; $^{\#\#}P$<0.05, $^{\#\#\#}P$<0.001, ASIA group compared with Oil group.

图6 积雪草苷减轻CCl_4诱导的小鼠肝纤维化

Fig.6 ASIA mitigates CCl_4-induced hepatic fibrosis in murine models

nanoparticles provide a new strategy for targeted delivery[22]. In follow-up research, we will focus on the targeting of ASIA to hepatic stellate cells.

Calcium ion (Ca^{2+}) is a ubiquitous intracellular signal in all eukaryotic organisms, capable of regulating many different processes, including proliferation, secretion, metabolism, fertilization[23]. Its influx and outflow in cells must be through special pumps and ion channels, which is also one of the necessary conditions for Ca^{2+} to function as a second messenger. Ca^{2+} signaling are closely linked to the pathogenesis and recuperation of liver fibrosis[24]. Intracellular Ca^{2+} signals upregulate the proliferation of HSC[25]. An earlier study has found that angiotensin II-induced activation of hepatic stellate cells by CD38-mediated Ca^{2+} signaling[26]. Endothelin and platelet-derived growth factor that two Ca^{2+} agonist hormones can activate hepatic stellate cells[25]. Inhibiting endothelin receptor-A by its antagonist Ambrisentan or LU 135252 decreases liver fibrosis in the rodent model[27-28]. PEI et al [29] recently discovered the putative targets for saffron, a medicine food homology herb, for the treatment of hepatic fibrosis is closely related to calcium signaling pathway through network pharmacology. We demonstrated that ASIA inhibited calcium signaling in the cytoplasm by downregulating calm and Fluo-4 AM. The main sources of intracellular Ca^{2+} are extracellular influx and intracellular ER storage. Mitochondria are one of the destinations of cytosolic Ca^{2+}. Our results shown that ASIA promotes mitochondrial calcium overload in HSC by Rhod-2 probe, and mitochondrial calcium channel blocker DIDS reversed the ASIA-induced cell death. It is imperative to understand how ASIA alters Ca^{2+} signaling.

A large body of literature indicates that there are interactions among calcium signaling, apoptosis, inflammation and oxidative stress during the occurrence and development of fibrosis[30-32]. Targeted regulation of any of these signaling pathways is also the mainstream approach for the fibrosis treatment. The level of calcium is essential to maintain the mitochondrial function. Activated calcium signaling pathway induced dysregulation of calcium homeostasis, which lead to mitochondrial dysfunction[33]. Mitochondrial pathway is one of the pathways that mediate apoptosis. The perturbation of intracellular calcium signaling pathway regulates apoptosis[34]. In seminal work on the NK-1R (neurokinin-1 receptor) produced by Fu's group, it is stated that NK-1R antagonists induce mitochondrial calcium overload, which leads to oxidative stress besides apoptosis in human leukemia cell[35]. WANG et al[36] reported that the pyrethroid pesticide Fenvalerate prompted calcium ions overload, induced production of ROS in the mitochondria, eventually lead to the apoptosis of hepatic cellular. Consistent with these findings, our researchs show that ASIA induced calcium overload and oxidative stress in mitochondrial, and HSC apoptosis. In another study, inhibition of Ca^{2+} signaling improved apoptosis in non-small cell lung cancer cells induced by Dolutegravir derivatives[34]. Besides, mitochondrial calcium overload exerts excessive mitochondrial ROS generation[37]. Increasing ROS levels also induced apoptosis. Schoenfisch and coworkers illustrated that melatonin drives apoptosis by elevating mitochondrial ROS generated in cancer cells[38]. In an interesting work by SONG's group, they found that drinking fructose increases level of oxidative stress, leading to liver inflammation/fibrosis[39]. More recently, LI et al[40] reported that ferroptosis inhibitor liproxstatin-1 significantly reduced the mitochondrial ROS content and liver fibrosis in metabolic dysfunction-associated fatty liver disease mice, which involve regulation of PANoptosis. Others have shown that glial proteins inhibit inflammatory macrophage activation to reduce steatosis and oxidative stress in non-alcoholic steatohepatitis and liver fibrosis mouse models[41]. Similar to the abovementioned results, our results also suggest that inhibition of inflammation contributed to the against fibrosis effect of ASIA. In a further attempt to determine the mechanisms by which ASIA exerts its regulation of apoptosis, inflammation and oxidative stress.

4 Conclusion

Taken together, we demonstrate that ASIA in-

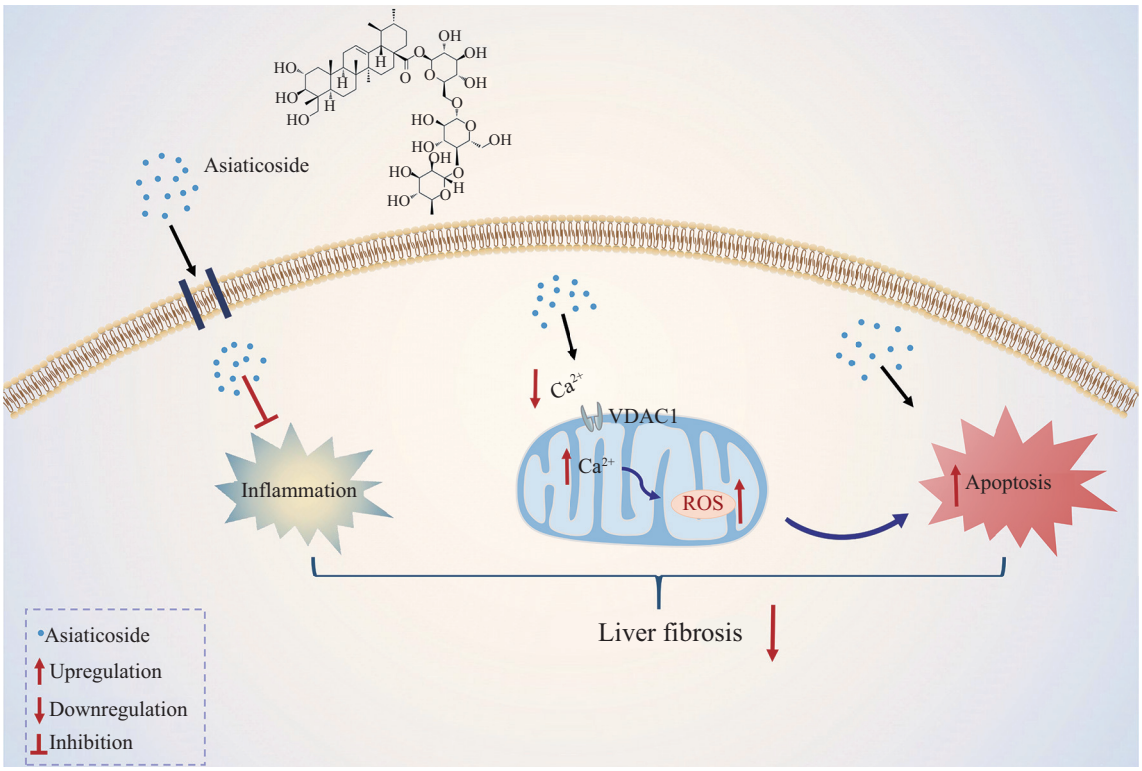

积雪草苷抑制炎症, 诱导胞质钙下调, 线粒体钙超载, 从而触发线粒体ROS水平升高, 促进肝星状细胞凋亡。

ASIA inhibits inflammation, induces cytoplasmic calcium down-regulation, mitochondrial calcium overload and triggers mitochondrial ROS rise to promote HSC apoptosis.

图7 积雪草苷改善肝纤维化的机制图

Fig.7 Mechanistic schematic of Asiaticoside ameliorates hepatic fibrosis

hibits HSCs activation dependent on calcium signaling pathways, which were associated with decreased cellular ROS, and the induction of apoptosis in HSC, thus attenuated CCl_4-induced liver fibrosis. We provide proof-of-concept that inhibition of calcium signaling pathways by ASIA or other pharmacologic agents that inhibited the pathways may be a promising strategy for anti-fibrosis therapy.

参考文献 (References)

[1] DAI X, DU Z, JIN C, et al. Inulin-like polysaccharide ABWW may impede CCl_4 induced hepatic stellate cell activation through mediating the FAK/PI3K/AKT signaling pathway *in vitro* & *in vivo* [J]. Carbohydr Polym, 2024, 326: 121637.

[2] YAN Z, CHENG X, WANG T, et al. Therapeutic potential for targeting Annexin A1 in fibrotic diseases [J]. Genes Dis, 2022, 9(6): 1493-505.

[3] HIGASHI T, FRIEDMAN S L, HOSHIDA Y. Hepatic stellate cells as key target in liver fibrosis [J]. Adv Drug Deliv Rev, 2017, 121: 27-42.

[4] YAN Z, WANG D, AN C, et al. The antimicrobial peptide YD attenuates inflammation via miR-155 targeting CASP12 during liver fibrosis [J]. Acta Pharm Sin B, 2021, 11(1): 100-11.

[5] LIN G, ZHONG Y, HU S, et al. Identification of (E)-1-((1H-indol-3-yl)methylene)-4-substitute-thiosemicarbazones as potential anti-hepatic fibrosis agents [J]. Bioorg Chem, 2024, 143: 107022.

[6] WANG X, ZHANG W, ZENG S, et al. Collagenase type I and probucol-loaded nanoparticles penetrate the extracellular matrix to target hepatic stellate cells for hepatic fibrosis therapy [J]. Acta Biomater, 2024, 175: 262-78.

[7] LIU Y, ZHAO J, MU X, et al. Asiaticoside-nitric oxide promoting diabetic wound healing through the miRNA-21-5p/TGF-β1/SMAD7/TIMP3 signaling pathway [J]. J Ethnopharmacol, 2024, 319(Pt 2): 117266.

[8] LIU S, CHEN L, LI J, et al. Asiaticoside mitigates alzheimer's disease pathology by attenuating inflammation and enhancing synaptic function [J]. Int J Mol Sci, 2023, 24(15): 11976.

[9] HU Z, WU T, ZHOU Z, et al. Asiaticoside attenuates blood-spinal cord barrier disruption by inhibiting endoplasmic reticulum stress in pericytes after spinal cord injury [J]. Mol Neurobiol, 2024, 61(2): 678-92.

[10] SUN J, TANG L, SHAN Y, et al. TMT quantitative proteomics and network pharmacology reveal the mechanism by which asiaticoside regulates the JAK2/STAT3 signaling pathway to inhibit peritoneal fibrosis [J]. J Ethnopharmacol, 2023, 309: 116343.

[11] LUO J, ZHANG T, ZHU C, et al. Asiaticoside might attenuate bleomycin-induced pulmonary fibrosis by activating cAMP and Rap1 signalling pathway assisted by A2AR [J]. J Cell Mol Med,

2020, 24(14): 8248-61.
[12] KOHLI S K, KHANNA K, BHARDWAJ R, et al. Assessment of subcellular ROS and NO metabolism in higher plants: multifunctional signaling molecules [J]. Antioxidants, 2019, 8(12): 641.
[13] BHATTACHARYYA A, CHATTOPADHYAY R, MITRA S, et al. Oxidative stress: an essential factor in the pathogenesis of gastrointestinal mucosal diseases [J]. Physiol Rev, 2014, 94(2): 329-54.
[14] TRUONG H T H, HO N T H, HO H N, et al. Morphological, phytochemical and genetic characterization of centella asiatica accessions collected throughout Vietnam and Laos [J]. Saudi J Biol Sci, 2024, 31(1): 103895.
[15] WITKOWSKA K, PACZKOWSKA-WALENDOWSKA M, PLECH T, et al. Chitosan-based hydrogels for controlled delivery of asiaticoside-rich centella asiatica extracts with wound healing potential [J]. Int J Mol Sci, 2023, 24(24): 17229.
[16] XU C, XIA L, XU D, et al. Cardioprotective effects of asiaticoside against diabetic cardiomyopathy: activation of the AMPK/Nrf2 pathway [J]. J Cell Mol Med, 2024, 28(2): e18055.
[17] HUANG X, JIA Z, LI X, et al. Asiaticoside hampers epithelial-mesenchymal transition by promoting PPARG expression and suppressing P2RX7-mediated TGF-β/Smad signaling in triple-negative breast cancer [J]. Phytother Res, 2023, 37(5): 1771-86.
[18] ZHANG L, LI H Z, GONG X, et al. Protective effects of asiaticoside on acute liver injury induced by lipopolysaccharide/D-galactosamine in mice [J]. Phytomedicine, 2010, 17(10): 811-9.
[19] WAN J, GONG X, JIANG R, et al. Antipyretic and anti-inflammatory effects of asiaticoside in lipopolysaccharide-treated rat through up-regulation of heme oxygenase-1 [J]. Phytother Res, 2013, 27(8): 1136-42.
[20] HUANG Q, ZHANG S, HUANG R, et al. Isolation and identification of an anti-hepatitis B virus compound from hydrocotyle sibthorpioides Lam [J]. J Ethnopharmacol, 2013, 150(2): 568-75.
[21] ZHANG M, LIU S, FANG L, et al. Asiaticoside inhibits renal fibrosis development by regulating the miR-142-5p/ACTN4 axis [J]. Biotechnol Appl Biochem, 2022, 69(1): 313-22.
[22] LIU C, GUO L, WANG Y, et al. Delivering metal ions by nanomaterials: turning metal ions into drug-like cancer theranostic agents [J]. Coord Chem Rev, 2023, 494: 215332.
[23] BERRIDGE M J. The inositol trisphosphate/calcium signaling pathway in health and disease [J]. Physiol Rev, 2016, 96(4): 1261-96.
[24] KRUGLOV E A, CORREA P R, ARORA G, et al. Molecular basis for calcium signaling in hepatic stellate cells [J]. Am J Physiol Gastrointest Liver Physiol, 2007, 292(4): G975-82.
[25] SOLIMAN E M, RODRIGUES M A, GOMES D A, et al. Intracellular calcium signals regulate growth of hepatic stellate cells via specific effects on cell cycle progression [J]. Cell Calcium, 2009, 45(3): 284-92.
[26] KIM S Y, CHO B H, KIM U H. CD38-mediated Ca^{2+} signaling contributes to angiotensin II-induced activation of hepatic stellate cells: attenuation of hepatic fibrosis by CD38 ablation [J]. J Biol Chem, 2010, 285(1): 576-82.
[27] OWEN T, CARPINO G, CHEN L, et al. Endothelin receptor-a inhibition decreases ductular reaction, liver fibrosis, and angiogenesis in a model of cholangitis [J]. Cell Mol Gastroenterol Hepatol, 2023, 16(4): 513-40.
[28] CHO J J, HOCHER B, HERBST H, et al. An oral endothelin-A receptor antagonist blocks collagen synthesis and deposition in advanced rat liver fibrosis [J]. Gastroenterology, 2000, 118(6): 1169-78.
[29] JIANG H, HUANG X, WANG J, et al. Hepatoprotective effect of medicine food homology flower saffron against CCl_4-induced liver fibrosis in mice via the Akt/HIF-1α/VEGF signaling pathway [J]. Molecules, 2023, 28(21): 7238.
[30] LI X, WANG Y, WANG H, et al. Endoplasmic reticulum stress is the crossroads of autophagy, inflammation, and apoptosis signaling pathways and participates in liver fibrosis [J]. Inflamm Res, 2015, 64(1): 1-7.
[31] KISSELEVA T, BRENNER D. Molecular and cellular mechanisms of liver fibrosis and its regression [J]. Nat Rev Gastroenterol Hepatol, 2021, 18(3): 151-66.
[32] CROSAS-MOLIST E, FABREGAT I. Role of NADPH oxidases in the redox biology of liver fibrosis [J]. Redox Biol, 2015, 6: 106-11.
[33] CHE Y, CHEN G, GUO Q, et al. Gut microbial metabolite butyrate improves anticancer therapy by regulating intracellular calcium homeostasis [J]. Hepatology, 2023, 78(1): 88-102.
[34] WANG W J, MAO L F, LAI H L, et al. Dolutegravir derivative inhibits proliferation and induces apoptosis of non-small cell lung cancer cells via calcium signaling pathway [J]. Pharmacol Res, 2020, 161: 105129.
[35] GE C, HUANG H, HUANG F, et al. Neurokinin-1 receptor is an effective target for treating leukemia by inducing oxidative stress through mitochondrial calcium overload [J]. Proc Natl Acad Sci USA, 2019, 116(39): 19635-45.
[36] QIU L L, WANG C, YAO S, et al. Fenvalerate induces oxidative hepatic lesions through an overload of intracellular calcium triggered by the ERK/IKK/NF-κB pathway [J]. Faseb J, 2019, 33(2): 2782-95.
[37] LI X, ZHANG W, CAO Q, et al. Mitochondrial dysfunction in fibrotic diseases [J]. Cell Death Discov, 2020, 6: 80.
[38] FLORIDO J, MARTINEZ-RUIZ L, RODRIGUEZ-SANTANA C, et al. Melatonin drives apoptosis in head and neck cancer by increasing mitochondrial ROS generated via reverse electron transport [J]. J Pineal Res, 2022, 73(3): e12824.
[39] CHO Y E, KIM D K, SEO W, et al. Fructose promotes leaky gut, endotoxemia, and liver fibrosis through ethanol-inducible cytochrome P450-2E1-mediated oxidative and nitrative stress [J]. Hepatology, 2021, 73(6): 2180-95.
[40] TONG J, LAN X T, ZHANG Z, et al. Ferroptosis inhibitor liproxstatin-1 alleviates metabolic dysfunction-associated fatty liver disease in mice: potential involvement of PANoptosis [J]. Acta Pharmacol Sin, 2023, 44(5): 1014-28.
[41] WANG X, HAUSDING M, WENG S Y, et al. Gliptins suppress inflammatory macrophage activation to mitigate inflammation, fibrosis, oxidative stress, and vascular dysfunction in models of nonalcoholic steatohepatitis and liver fibrosis [J]. Antioxid Redox Signal, 2018, 28(2): 87-109.